Path Tracking of a Bi-steerable Mobile Robot: An Adaptive Off-road Multi-control Law Strategy

Roland Lenain[1], Ange Nizard[2], Mathieu Deremetz[1], Benoit Thuilot[2], Vianney Papot[1] and Christophe Cariou[1]

[1]*Irstea, Technologies and Information Support System Research Unit, 9 avenue Blaise Pascal, CS 20085, 63178 Aubière, France*

[2]*Université Clermont Auvergne, CNRS, SIGMA Clermont, Institut Pascal, F-63000 Clermont-Ferrand, France*

Keywords: Adaptive Control, Four-wheel-steering Mobile Robot, Path Following, Agriculture, Off-road.

Abstract: This paper proposes a path tracking control algorithm dedicated to off-road mobile robots equipped with two steering axles. Four wheel steering mobile robot allows to enhanced motion capability with respect to classical car-like mobile robot, while reducing the friction induced by the skid-steered architecture. In particular, such a kinematic structure makes it possible to independently control the robot heading and its position, or to increase turning capabilities. In this paper, a strategy is developed in order to reduce the space required when achieving manoeuvres around a desired trajectory. Contrarily to classical point of view, expressing a relationship between the front and rear wheels, the control laws here proposed aim at following the same path for the front and the rear centre of the axle. The robot is then split into two subsystems, regulating two lateral deviations with respect to a desired trajectory.

1 INTRODUCTION

The potentialities of mobile robotics in various field of application are more and more considered, since they meet social needs in terms of comfort, safety, and reliability. In particular, transportation and industrial mobile robots are the subject of a growing interest with several commercial autonomous devices (Lefvre et al., 2015). The social demand is particularly pregnant in off-road application (such as environment and agriculture (Blackmore, 2014)), where hazardous situations may be encountered, or where human drivers may be exposed to dangerous products. Nevertheless, the motion has to be accurately controlled, even when the robot is submitted to perturbations with respect to classical assumptions achieved in literature (such as the rolling without sliding or ideal actuators). Moreover, the robots have to move in crowded environments with restricted areas to achieve manoeuvres. Basically, manually driven vehicles are equipped with additional degrees of freedom to increase their agility. Regarding mobile robotics, the raise of unmanned adaptable robots equipped with four independent steering wheels (also called 4WS robots) having a huge range of movement such as the Thorvald platform (Grimstad et al., 2015) or the agricultural robot proposed in (Haibo et al., 2015), allows to imagine that new kinds of movement during path tracking can be achieved, such as the reduction of the radius of curvature when moving in a warehouse where a lot of goods are stored or in agricultural field for reducing headlands.

The control of 4WS robots is often made by imposing a rear steering angle as a function of front steering angle, as proposed in (Wang and Qi, 2001) and in (Peng et al., 2004). If this improves the turning capability of the robot (Ackermann, 1994), this does not necessarily minimizes the space required for manoeuvres. Some other works take advantages of having two steering angles to control independently the position and the heading of a mobile robot with respect to the trajectory (Cariou et al., 2009) or in the global frame (Deremetz et al., 2017a) or to control each axle for tracking a "dual-path" (Nizard et al., 2016) . These attractive features permit to preserve for instance the orientation with respect to a slope, or to compensate for the drift when moving fast. If the position and the orientation of the robot, around a desired trajectory, have to be controlled to optimize manoeuvres, we propose in this paper a new approach to

Lenain, R., Nizard, A., Deremetz, M., Thuilot, B., Papot, V. and Cariou, C.
Path Tracking of a Bi-steerable Mobile Robot: An Adaptive Off-road Multi-control Law Strategy.
DOI: 10.5220/0006865801630170
In *Proceedings of the 15th International Conference on Informatics in Control, Automation and Robotics (ICINCO 2018) - Volume 2*, pages 163-170
ISBN: 978-989-758-321-6

control the front axle and the rear axle, independently, to ensure their passages by the same path.

These works are achieved in the framework of path tracking task (Raksincharoensak et al., 2001). Basically, a path is preliminary defined and a reference point on the robot has to follow this trajectory (which is usually chosen as the middle of the rear axle for a car like mobile robot, for interesting properties see (Campion et al., 1996)). When only the front steering angle is actuated, the middle of the front axle is necessarily outside of the turn. In this paper, robot is viewed as two subsystems (front and rear), with a control laws independently servoing the rear and the front position. This permits to ensure that two control points of the robots (the middle of two front wheels and the middle of two rear wheels) will follow accurately the same trajectory. The control is based on the assumption that the kinematic description of robot motion may be split into two models. One describes the motion of rear axle, and the other is dedicated to the front of the robot. These two models are only linked by the rear steering variables, which can be viewed as measured parameters for the front semi-model. This point of view relies on an extended kinematic model, allowing to account for non perfect conditions thanks to models-based adaptive algorithm (Anderson and Bevly, 2005). This approach then permits to derive independently two control laws for front and rear steering angles. As a result, two points on the robot are tracking the same trajectory.

The paper is organized as follows. First, the modelling of the robot is proposed, based on an extended kinematic approach, recalled in the paper. The online estimation of variables required is then briefly detailed in a second section, using observation techniques. This observer permits to know all the variables introduced in the model. As a result, the model may be used to build two independent control laws, which are derived in a third section. The performances of the proposed approach are then tested by performing full scale experiments on an off-road mobile robot. They permits to highlight the efficiency of the proposed algorithm.

2 MODELING OF THE ROBOT

2.1 Assumptions and Notations

This paper considers a two-wheel steering mobile robot. As is commonly perceived in the framework of path tracking (see (Morin and Samson, 2000)), the robot is considered as symmetric along its heading, and its four wheels are supposed to be in contact with the ground. As a result, the robot may be viewed as a bicycle with an equivalent front steering angle δ_F, an equivalent rear steering angle δ_R and a wheelbase L. This point of view is depicted in Fig. 1.

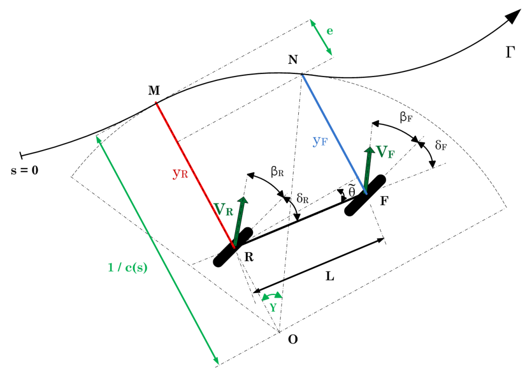

Figure 1: Extended kinematic model of the robot with respect to the reference trajectory Γ.

This robot of class {1,2}, according to the classification proposed by (Campion et al., 1996), is controlled thanks to its rear velocity v_R, dependent on the wheel rotations, and the two steering angles : δ_F for the front axle, and δ_R for the rear one. Classically, the motion model is build under the rolling without sliding assumption, imposing that the direction of each speed vector is parallel to the tires. In off-road contexts, such an assumption is not valid, due to slippages. As a result, the orientation of speed vectors are different from the tire orientations (Canudas-de Wit et al., 2001). An angle appears for each virtual wheel (front and rear), which is named sideslip angle and are denoted in this paper by β_F for the front wheel and β_R for the rear one. These two angles are hardly measurable directly and are assumed to be estimated indirectly by the observer described in Sec. 3.

Assuming that sideslip angles are known, the front and rear steering angles are considered to be the control variables of the system, since the velocity v_R is considered as a measured parameter, potentially varying. Thanks to this control variables, the objective of a path tracking control law is to impose the convergence of the robot w.r.t. the desired path Γ (see Fig. 1). The tracking error y_R is basically defined as the minimal distance between the middle of the rear axle R to Γ. $\tilde{\theta}$ is the angular deviation, denoting the difference between the robot's heading θ and the orientation of the trajectory at the closest point of R belonging to Γ. At this point, one can define the curvilinear abscissa s on the path to be followed.

In this paper, we consider a second lateral deviation with respect to the middle of the front axle (point F). The distance between F and Γ is called the front lateral deviation and is denoted by y_F. In this paper, we consider that the wheelbase L (distance between F and R) is small with respect to the curvature of the reference path at point *M* (denoted by c(s)). As a result, the path to be followed may locally be approximated by a circle whose radius is $\frac{1}{c(s)}$ and whose centre is O. In this paper, we consider a second lateral deviation w.r.t. the middle of the front axle (point F), denoted y_F. We consider that the intersection between the straight line parallel to (MR) passing through the point F, and the reference path Γ, is denoted N.

2.2 Global Motion Equations

As has been detailed in detailed in (Yi et al., 2009) for the extended model depicted in Fig. 1, the motion equation for the classical path tracking problem may be expressed as:

$$\left\{\begin{array}{lcl} \dot{s} & = & v_R \dfrac{\cos(\tilde{\theta}_2)}{1-c(s)\,y_R}, \\ \dot{y}_R & = & v_R \sin(\tilde{\theta}_2), \\ \dot{\tilde{\theta}} & = & v_R \left[\cos(\delta_R+\beta_R)\,\lambda_1-\lambda_2\right], \end{array}\right. \quad (1)$$

with:

$$\left\{\begin{array}{lcl} \lambda_1 & = & \dfrac{\tan(\delta_F+\beta_F)-\tan(\delta_R+\beta_R)}{L}, \\ \lambda_2 & = & \dfrac{c(s)\cos(\tilde{\theta}+\delta_R+\beta_R)}{1-c(s)\,y_R}, \\ \tilde{\theta}_2 & = & \tilde{\theta}+\delta_R+\beta_R. \end{array}\right. \quad (2)$$

This model is suitable for the path tracking approach since it can be turned into a linear form as has been shown in (Morin and Samson, 2000), since the extension to sideslip angles preserve the kinematical structure of mobile robots. As has been achieved in (Lenain et al., 2010), this model permits to derive a control law enabling the convergence of the rear lateral deviation y_R to zero. In particular, this is possible whatever the value of the rear steering angle δ_R, provided that its time derivative $\dot{\delta}_R$ can be neglected with respect to the settling time of the control law imposed on the front steering angle δ_F. In the previous cited reference, the rear steering angle is then used to control an angular deviation. If this permits to control the heading of a robot independently from its lateral position, it does not ensure explicitly the control of the front axle position. As this paper aims at ensuring the convergence of the position of the front and the rear axle (point R and F) to the reference path Γ, an additional model has to be introduced.

2.3 Modeling of the Two Subsystems

In order to ensure that both points of the robot chassis F and R follow the same trajectory Γ, two models for the derivative of tracking errors y_F and y_R are developed from the representation depicted in Fig. 1. The dynamic of the rear lateral deviation y_R is obtained directly from the classical set of equation (2), i.e:

$$\dot{y}_R = v_R \sin(\tilde{\theta}_2)\,. \quad (3)$$

Regarding the front axle, let us consider the geometric properties in order to derive an expression of y_F with respect to y_R. From Fig. 1, one can define the relation (4),

$$y_F = y_R + L\sin(\tilde{\theta}) + e\,. \quad (4)$$

In this equation, only the deviation e remains unknown. Assuming that, at each step, the trajectory is locally (at any curvilinear abscissa s) viewed as a circle of radius $\frac{1}{c(s)}$, e can be expressed as:

$$e = \frac{1-\cos(\gamma)}{c(s)}, \quad (5)$$

where γ, depicted in Fig. 1 is the angle defined by the points [M O N]. This angle may be easily obtained using the radius of curvature of the reference trajectory, the angular deviation $\tilde{\theta}$ and the robot wheelbase L:

$$\gamma = \arcsin(L\,c(s)\cos(\tilde{\theta}))\,. \quad (6)$$

Thanks to this relation, the distance e is entirely known and the lateral front deviation may be computed thanks to the relation (2). The time derivative may then be obtained, considering that e is slowly varying with respect to the possible variation of y_F thanks to actuator reactivity. It comes:

$$\dot{y}_F = \dot{y}_R + L\dot{\tilde{\theta}}\cos(\tilde{\theta})\,. \quad (7)$$

Using the global model, one can define an explicit expression for the evolution of front lateral deviation:

$$\dot{y}_F = v_R \sin(\tilde{\theta}_2) + L\,v_R\cos(\tilde{\theta})\left[\cos(\delta_R+\beta_R)\,\lambda_1-\lambda_2\right]. \quad (8)$$

The definition of λ_1 and λ_2 given in the model (2) are explicitly linked to the control variable δ_F and δ_R. Thanks to equations (3) and (2.3), the relationships between the control variables and the time derivatives of the lateral deviations are available. This constitutes the model which will be used in Sec. 4 to derive the control laws, provided that the sideslip angles β_F and β_R are known, which is the aim of the observer described hereafter.

3 OBSERVATION OF SIDESLIP ANGLES

In order to derive control laws for the convergence of the lateral errors to zero, the knowledge of sideslip angles is mandatory. There is no perception systems allowing to measure directly such variables. Nevertheless, we assume that sensors on-boarded on the robot permit to measure the position, the orientation and the velocity of the robot at a given point, here R. As it has been shown in (Lenain et al., 2014) and extended to higher dynamic phenomena in (Deremetz et al., 2017b), an observer may be built in order to estimate the two sideslip angles thanks to such a perception system. The details of the computation are in the previous references. In this paper, the same approach is used and only a short presentation is hereafter proposed.

3.1 Observer State

In order to achieve the indirect estimation of sideslip angles, let us consider the state space model ξ composed of the robot lateral position and relative orientation. Its evolution may be written as (9), based on the model (2).

$$\dot{\xi} \quad = \quad \begin{bmatrix} \dot{\xi}_{dev} \\ \dot{\xi}_{\beta} \end{bmatrix} \quad = \quad \begin{bmatrix} f(\xi_{dev},\xi_{\beta},v_R,\delta_F,\delta_R) \\ 0_{2\times 1} \end{bmatrix}, \tag{9}$$

where ξ is split into two sub-states:

- $\xi_{dev} = [y \quad \tilde{\theta}]^{T}$, which constitutes the deviations of the robot with respect to the trajectory Γ,
- $\xi_{\beta} = [\beta_F \quad \beta_R]^{T}$, which is composed of the sideslip angles, to be estimated.

The function $f(\xi_{dev},\xi_{\beta},v_R,\delta_F,\delta_R)$ is constituted of the two last lines of the system (2). Because no equation is available for the evolution of $\dot{\beta}_F$ and $\dot{\beta}_R$ in a kinematic representation, it is set to $0_{2\times 1}$. If the observer gains are chosen appropriately, this modeling assumption is admissible, as it has been shown in (Lenain et al., 2014). The objective of the observer is to ensure the convergence of the complete observed state $\hat{\xi}$ to the actual ξ, measuring only the sub-state ξ_{dev}. As a result only the observation error related to the deviation $\tilde{\xi}_{dev} = \hat{\xi}_{dev} - \xi_{dev}$ is known.

3.2 Observer Equations

It has been shown in (Lenain et al., 2014) that the observer defined by equation (10) permits the convergence of the whole observed state $\hat{\xi}$ to the actual one ξ.

$$\begin{cases} \dot{\hat{\xi}}_{dev} & = \quad f(\xi_{dev},\hat{\xi}_{\beta},v_R,\delta_F,\delta_R) + \alpha_{dev}(\tilde{\xi}_{dev}), \\ \dot{\hat{\xi}}_{\beta} & = \quad \alpha_{\beta}(\tilde{\xi}_{dev}), \end{cases} \tag{10}$$

where α_{dev} and α_{β} are two functions of the observation error attached to the deviation part of the state ξ, and defined as follows:

$$\begin{cases} \alpha_{dev}(\tilde{\xi}_{dev}) & = \quad K_{dev}\tilde{\xi}_{dev}, \\ \alpha_{\beta}(\tilde{\xi}_{dev}) & = \quad K_{\beta}\left[\frac{\partial f}{\partial \hat{\xi}_{\beta}}(\xi_{dev},\hat{\xi}_{\beta},v_R,\delta_F,\delta_R)\right]^{T}\tilde{\xi}_{dev}, \end{cases} \tag{11}$$

with K_{dev} a 2×2 positive diagonal matrix and K_{β} a positive scalar. These gains permit to tune the settling time of the observer. As it can be seen considering (11), only the measurable error $\tilde{\xi}_{dev}$ is mandatory to compute the proposed observer. Thanks to this approach, the global model (2) may be entirely known. As a consequence, expressions of front and rear lateral deviation derivative (3) and (2.3) can be used to compute control laws for the path tracking of points F and R.

4 CONTROL LAWS

Thanks to the modeling proposed previously and the observer defined in (Lenain et al., 2014) and briefly presented in the previous section, a model linking lateral deviations (front y_F and rear y_R) to the control variables (steering angles and velocity) is available. As a consequence, control laws on steering angles, considering the velocity v_R as a measured parameter are here developed. This is achieved considering two subsystems controlled by each steering angle.

4.1 Rear Steering Angle

Let us first consider the regulation of the rear control point R on the trajectory. The objective is to ensure the convergence of the rear lateral deviation y_R to zero. The evolution of y_R is related to the rear steering angle by the model (3), thanks to the intermediate variable $\tilde{\theta}_2$. The convergence $y_R \to 0$ may be ensured by imposing the following differential equation:

$$\dot{y}_R \quad = \quad -K_R\, y_R, \tag{12}$$

with K_R a positive scalar defining the settling time for the exponential convergence of y_R to zero imposed by (12). By injecting in this condition the expression of rear lateral error derivative (3), and using the definition of $\tilde{\theta}_2$, one can reformulate the previous conditions as:

$$\delta_R \quad = \quad \arcsin\left(\frac{-\mathrm{K}_R\, \mathrm{y}_R}{\mathrm{v}_R}\right) - \tilde{\theta} - \hat{\beta}_R\,, \qquad (13)$$

provided that $\mathrm{v}_R \neq 0$ and $\mid \frac{-\mathrm{K}_R\, \mathrm{y}_R}{\mathrm{v}_R} \mid < 1$. In practice, in path tracking the velocity is always positive and consequently non null, since the robot cannot be controlled to its desired trajectory if it is stopped. Nevertheless, in order to permit stopping points to the robot, one can define the gain K_R as a function of velocity, which has to be null when $\mathrm{v}_R = 0$. The second conditions is linked to the existence range of the function arcsin. This impose that lateral error is small enough with respect to the robot velocity and the gain: $\mid \mathrm{y}_R \mid < \frac{\mid \mathrm{v}_R \mid}{\mathrm{K}_R}$. In practice, according to the values usually reached by velocity and the choice for the control gain, the lateral deviation has to exceed several meters in order to come across a singularity. When properly initialized, such a value may hardly be reached. Nevertheless, a saturation on error, or a variable gain may be computed in order to avoid such a singularity.

The expression (13) constitutes the control law on the rear steering angle in order to ensure the differential equation (12) on lateral deviation y_R, implying its convergence to zero.

4.2 Front Steering Angle

Once the rear steering angle is computed thanks to the control law (13), the objective is to derive a control law for front steering in order to ensures the convergence of the front steering (denoted by the point F in Fig. 1) axle to the desired trajectory Γ. In other words, the objective is to ensure the convergence of the front lateral deviation to zero $\mathrm{y}_F \to 0$. Thanks to the extended kinematic model computation, the expression (2.3) is available for the time derivative of y_F, pending on sideslip angles and steering angles. One possible condition on $\dot{\mathrm{y}}_F$ in order to permit the convergence of y_F to zero may be defined as follows.

$$\dot{\mathrm{y}}_F \quad = \quad -\mathrm{K}_F\, \mathrm{y}_F\,, \qquad (14)$$

provided that K_F is a positive scalar, the condition (14) will lead the front lateral error to exponentially converge to zero. As rear steering angle δ_R is known, as well as sideslip angles ($\hat{\beta}_F$ and $\hat{\beta}_R$ are indeed on-line estimated thanks to the observer (10)), one can introduce the explicit expression (2.3) for $\dot{\mathrm{y}}_F$ in the previous condition. Computation permits to extract the following expression for front steering angle.

$$\delta_F = \arctan\left\{\frac{\mathrm{L}\,\lambda_2}{\cos(\delta_R+\hat{\beta}_R)} - \frac{\mathrm{K}_F\, \mathrm{y}_F}{\mathrm{v}_R \cos(\delta_R+\hat{\beta}_R)\cos(\tilde{\theta})} - B_1\right\} - \hat{\beta}_F\,, \qquad (15)$$

with $B_1 = \frac{\sin(\tilde{\theta}_2)}{\cos(\delta_R+\hat{\beta}_R)\cos\tilde{\theta}} - \tan(\delta_R+\hat{\beta}_R)$,

λ_1 and λ_2 that are already defined by the model (2), replacing sideslip angles by their corresponding observation values (i.e. $\hat{\beta}_{\{F,R\}}$ instead of $\beta_{\{F,R\}}$). This control law for front steering angle exists under the same conditions than those defined for rear steering control law. It has been designed using front and rear kinematic models defined in Sec. 2, under the assumption that the derivative of the rear sideslip angle and the derivative of the rear steering angle are defined as : $(\dot{\beta}_F, \dot{\delta}_R) = (0,0)$. Such an assumption is considered to be reasonable since the tuning of gain K_F and K_R can be achieved on this way (i.e. $\mathrm{K}_F > \mathrm{K}_R$). This setting permits to emphasize reactivity of front axle with respect to the rear one in order to meet such an assumption. As pointed out in experimental results, it does not affect the performances of the proposed algorithm.

5 EXPERIMENTAL RESULTS

5.1 Experimental Setup

The four wheel-driven robot depicted in Fig. 2 is used in order to point out the result of the proposed approach. It is a fully electric mobile robot equipped with four independent motors controlling wheels speed. Two additionnal motors regulate the front and rear steering angles. As shown in Fig. 2, the main on-boarded sensor is an RTK-GPS settled on the vertical of the rear axle (above the point R depicted in Fig. 1). It supplies the position within an accuracy of ± 2cm, while the heading is computed thanks to a Kalman filter, mixing the GPS heading data and the robot odometry. Related to the definition of a reference path, these data permits to feed both the observer, and the control laws (13) and (4.2). In order to show the efficiency of the proposed control algorithm, the autonomous tracking of the path depicted in Fig. 3 is first realize by the robot using only the front steering angle axle. The control in this case is the approach proposed in previous works (Lenain et al., 2014), based on the same observer, and using predictive features.

Figure 2: Experimental robot and on-boarded sensor.

In order to highlight the benefit of the proposed four-wheel-steering control strategy, the reference trajectory, depicted in black line in Fig. 3, has been previously recorded. This path, starting in A and ending in B, is composed of straight line parts at the beginning and the end, separated by two successive curves with a radius of curvature equal to 3.4m and 3m respectively. Such radii cannot be reached in practice when controlling only the front steering wheels (limited to an angle of 20°). As a result, the front steering angle saturates and the robot cannot follow the trajectory properly. This is pointed out by considering the result of the path tracking depicted in red in Fig. 3, achieved at 2m.s^{-1}, with only the front steering activated.

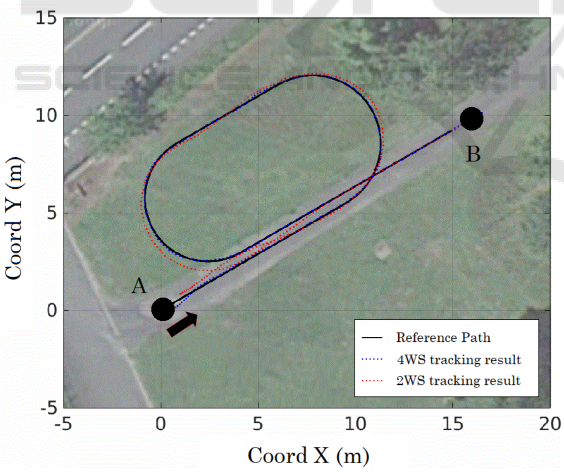

Figure 3: Path to be followed and actually achieved trajectories.

On the contrary, when using the front and rear steering control strategy proposed in that paper, the robot is able to track accurately the trajectory. The successive positions recorded at 2m.s^{-1}, when using control laws (13) and (4.2) are indeed reported in blue in Fig. 3, which are superimposed with the desired trajectory.

5.2 Manoeuvrability Improvement in Tracking Accuracy

The tracking accuracy obtained with and without using the control of the rear steering angle may be investigated in Fig. 4. The red dashed line depicts the tracking error obtained when controlling only the front steering axle. The large error obtained during the curves (between curvilinear abscissa 15-25m and 30-42m) are due to the saturation of the front steering axle, as reported in Fig. 5.

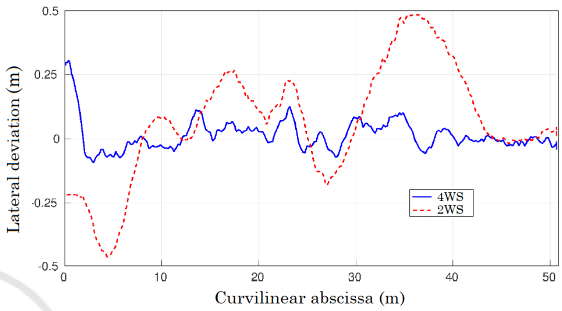

Figure 4: Comparison of tracking errors with and without the use of rear steering angle.

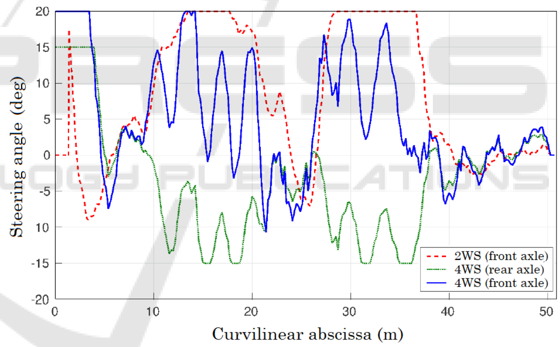

Figure 5: Comparison of front steering angles, and rear steering angle when used.

In this figure, the front steering angle obtained when controlling the robot only with front steering wheels is reported in dashed red line. It can be noticed that the saturation value of 20° is obtained almost all the two bends. On the contrary, when using the front and rear steering wheels, the front steering angle (depicted in blue plain line) is decreased thanks to the rear steering angle (turning to the right), depicted in green dotted line.

This permits to the robot to stay on the trajectory, since the lateral deviation obtained when using the proposed control strategy stay around zero, whatever the curvature of the desired trajectory and the type of ground (alternatively gravel and wet grass). This tracking error is indeed depicted in blue plain line in Fig. 4 and stays within $\pm 10cm$.

5.3 Trajectory of Each Axle

The second benefit of this approach lies in the reduction of the space occupied by the robot during manoeuvers, since front and rear axle follow the same trajectory during the bend. This can be verified in Fig. 6, where the trajectory of the front axle (point F) is depicted in green dotted line (in addition to the reference trajectory depicted in black and the position of point R depicted in blue).

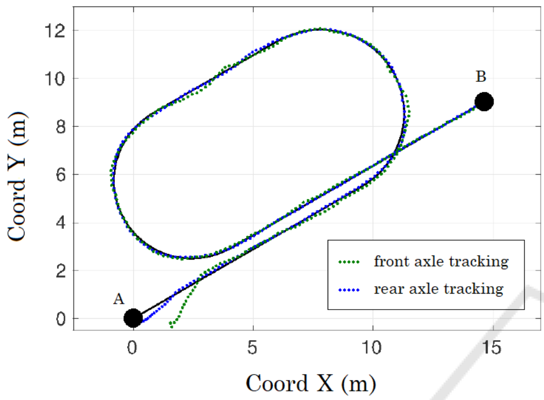

Figure 6: Path to be followed and actually achieved trajectories.

One can see that each point of the robot (R and F) follows accurately the trajectory instead of having a deviation in the front axle when using a single steering axle robot. This permits to reduce the necessary space to achieve harsh manoeuvres by increasing the turning capabilities. As it can be seen on the videos attached to the paper, using such an algorithm, the robot is able to reach the trajectory without having an angular deviation. During initialization phases, the front and rear steering angles indeed rotate in the same direction to cancel the initial lateral deviation.

In order to point out the accuracy obtained during the tracking the Tab. 1 shows the statistical data related to the absolute values of lateral deviations obtained during the tracking. The mean and standard deviation of the absolute value of the error recorder at points R (y_R) and F (y_F) are reported for the tracking results using the proposed approach and compared to the data obtained using the front steering angle. It can be noticed that when using the proposed approach, the mean and standard deviations are very close to zero (a few centimetres accuracy), despite of the harsh radius of curvature imposed by the path to be followed. On the contrary, when using a single steering axle (front), since saturations occurred, large deviations may be recorded leading to a bad accuracy (with a mean of more than 30cm, for the front steering point). This value is logicallly bigger than for the rear control point R (22cm) since only the position of point R is controlled when a single steering angle is controlled.

Table 1: Comparison of absolute value of lateral deviation recorded during the tracking.

	2 steering angles		1 steering angle	
	$\mid y_R \mid$	$\mid y_F \mid$	$\mid y_R \mid$	$\mid y_F \mid$
mean (m)	0.04	0.07	0.22	0.32
standard deviation (m)	0.03	0.05	0.19	0.27

When using the proposed control laws (13) and (4.2), it can be noticed than the front lateral deviation y_F is a little bit less accurate than the rear one y_R (7cm against 4cm). This is due to the small deviations of the point F which can be noticed in Fig. 6. This can be explained by the fact that the control law for the front steering angle (4.2) does not account for the variations of rear steering angle δ_R. When fast variations of δ_R occurs, a settling time is mandatory for the front axle to compensate for these variations. As a results, some punvtual overshoots can be recorder. This may be tackled in future works by using predictive control.

6 CONCLUSIONS

In this paper a new control algorithm dedicated to four wheel-driven mobile robot is proposed. The front and rear axle of the robot are considered as two independent sub-systems regulating their own point on the same desired trajectory. The physical link is ensured by the computation of the front tracking error, which is deduced from the rear position and the robot's heading. An adaptive approach is added from previous work in order to face the potential influence of bad grip conditions, since such works are devoted to off-road application, such as in civil security or in agriculture, for which high manoeuvrability is mandatory.
Experimental results have shown the efficiency of the proposed approach at low speed (up to $2 m.s^{-1}$), for which the dynamical effects can be neglected. Future works are focused on the increase of the robot speed. A predictive layer, exploiting the knowledge of the path to be followed is expected to be implemented to compensate for inertial effects and the influence of low level delays. Moreover, control laws proposed explicitly relies on the velocity and do not exist when the robot stops. This impose to switch the control laws to zero when the velocity is close to zero. To overcome this drawback, a new version will be proposed, based on a model using partial derivative of error with respect to curvilinear abscissa, instead of time derivatives.

ACKNOWLEDGEMENTS

This work has been sponsored by the French government research program "Investissements d'Avenir" through the IMobS3 Laboratory of Excellence (ANR-10-LABX-16-01), by the European Union through the program "Regional competitiveness and employment 2007-2013" (ERDF Auvergne region), and by the Auvergne region.
It received the support of French National Research Agency under the grant number ANR-14-CE27-0004 attributed to Adap2E project (adap2e.irstea.fr) and has also been sponsored through the RobotEx Equipment of Excellence (ANR-10-EQPX-44). We thank them for their financial support.

REFERENCES

Ackermann, J. (1994). Robust decoupling, ideal steering dynamics and yaw stabilization of 4ws cars. *Automatica*, 30(11):1761–1768.

Anderson, R. and Bevly, D. (2005). Estimation of tire cornering stiffness using GPS to improve model based estimation of vehicle states. In *IEEE Intelligent Vehicles Conference*, Las Vegas, U.S.A.

Blackmore, C. (2014). Learning to change farming and water management practices in response to the challenges of climate change and sustainability. *Outlook on AGRICULTURE*, 43(3):173–178.

Campion, G., Bastin, G., and Andréa-Novel, B. d. (1996). Structural properties and classification of kinematic and dynamic models of wheeled mobile robots. *IEEE Transactions on Robotics and Automation*, 12(1):47–62.

Canudas-de Wit, C., Tsiotras, P., Claeys, X., Yi, J., and Horowitz, R. (2001). Friction tire/road modeling, estimation and optimal braking control. In *NACO2 Workshop, Lund, Sweden*, volume 45.

Cariou, C., Lenain, R., Thuilot, B., and Berducat, M. (2009). Automatic guidance of a four-wheel-steering mobile robot for accurate field operations. *Journal of Field Robotics*, 26(6-7):504–518.

Deremetz, M., Lenain, R., Couvent, A., Cariou, C., and Thuilot, B. (2017a). Path tracking of a four-wheel steering mobile robot: A robust off-road parallel steering strategy. In *Mobile Robots (ECMR), 2017 European Conference on*, pages 1–7. IEEE.

Deremetz, M., Lenain, R., Thuilot, B., and Rousseau, V. (2017b). Adaptive trajectory control of off-road mobile robots: A multi-model observer approach. In *Robotics and Automation (ICRA), 2017 IEEE International Conference on*, pages 4407–4413. IEEE.

Grimstad, L., Pham, C. D., Phan, H. T., and From, P. J. (2015). On the design of a low-cost, light-weight, and highly versatile agricultural robot. In *Advanced Robotics and its Social Impacts (ARSO), 2015 IEEE International Workshop on*, pages 1–6. IEEE.

Haibo, L., Shuliang, D., Zunmin, L., and Chuijie, Y. (2015). Study and experiment on a wheat precision seeding robot. *Journal of Robotics*, 2015:12.

Lefvre, S., Carvalho, A., and Borrelli, F. (2015). Autonomous Car Following: A Learning-Based Approach. *IEEE Intelligent Vehicles \ldots*.

Lenain, R., Thuilot, B., Cariou, C., and Martinet, P. (2010). Mixed kinematic and dynamic sideslip angle observer for accurate control of fast off-road mobile robots. *Journal of Field Robotics*, 27(2):181–196.

Lenain, R., Thuilot, B., Guillet, A., and Benet, B. (2014). Accurate target tracking control for a mobile robot: a robust adaptive approach for off-road motion. In *IEEE International Conference on Robotics and Automation (ICRA)*.

Morin, P. and Samson, C. (2000). Practical stabilization of a class of nonlinear systems. Application to chain systems and mobile robots. In *IEEE Conference on Decision and Control (CDC)*, volume 3, pages 2989–2994, Sydney (Australia).

Nizard, A., Thuilot, B., Lenain, R., and Mezouar, Y. (2016). Nonlinear path tracking controller for bi-steerable vehicles in cluttered environments. *IFAC-PapersOnLine*, 49(15):19–24.

Peng, S.-T. P. S.-T., Sheu, J.-J. S. J.-J., and Chang, C.-C. C. C.-C. (2004). A control scheme for automatic path tracking of vehicles subject to wheel slip constraint. In *Proceedings of the 2004 American Control Conference*, volume 1, pages 804–809 vol.1.

Raksincharoensak, P., Nagai, M., and Mouri, H. (2001). Investigation of automatic path tracking control using four-wheel steering vehicle. In *IVEC2001. Proceedings of the IEEE International Vehicle Electronics Conference 2001. IVEC 2001 (Cat. No.01EX522)*, pages 73–77.

Wang, D. and Qi, F. (2001). Trajectory planning for a four-wheel-steering vehicle. In *Robotics and Automation, 2001. Proceedings 2001 ICRA. IEEE International Conference on*, volume 4, pages 3320–3325. IEEE.

Yi, J., Wang, H., Zhang, J., Song, D., Jayasuriya, S., and Liu, J. (2009). Kinematic modeling and analysis of skid-steered mobile robots with applications to low-cost inertial-measurement-unit-based motion estimation. *IEEE Transactions on Robotics*, 25(5):1087–1097.